Quasi-Elastic Light Scattering of Gelatin Solutions and Gels

Eric J. Amis, Paul A. Janmey, John D. Ferry,* and Hyuk Yu

Department of Chemistry, University of Wisconsin, Madison, Wisconsin 53706.
Received June 11, 1982

ABSTRACT: Quasi-elastic light scattering measurements have been made on aqueous solutions of gelatin (number-average molecular weight 35 000) at 35 °C, above the melting temperature, at concentrations from 2 to 20% by weight and on gels with 15% concentration over a range of temperature and solvent viscosity (adjusted by incorporation of glycerol). In the gels, the dynamic scattering was analyzed in terms of a single decay process, which was identified with the mutual diffusion coefficient, D_c. The value of D_c was about 430 $\times 10^{-9}$ cm^2/s in water, and it was found to be inversely proportional to solvent viscosity over a range of 3 orders of magnitude. In the solutions, measurements over a wide range of sample times revealed two decay processes. The fast process provided a diffusion coefficient with the same magnitude as D_c in aqueous gels, identified as the mutual diffusion coefficient, which increased with concentration c (in g/cm^3) with about the 0.3 power. The slow process provided a much smaller diffusion coefficient ((0.7–39) $\times 10^{-9}$ cm^2/s), which decreased sharply with increasing concentration, and was identified with the self-diffusion coefficient of the gelatin, D_2. The magnitude of D_2 agreed with that calculated from the monomeric friction coefficient ζ_0 obtained from viscoelastic measurements on gels of the same gelatin.

Measurements of quasi-elastic light scattering by photon correlation spectroscopy of concentrated polymer solutions and gels provide values of a mutual (cooperative) diffusion coefficient D_c, which is a measure of the rate of relaxation of local concentration gradients.[1] In several cases where a concentrated or semidilute uncross-linked polymer solution has been compared with a cross-linked gel having identical or nearly identical chemical structure and the same polymer concentration, the mutual diffusion coefficients are the same[2] or closely similar.[3,4] This corresponds to the conclusion from viscoelastic properties that the monomeric friction coefficient ζ_0, reflecting motions of a few monomer units together, is essentially unaffected by the presence of widely spaced cross-links.[5] However, it should be pointed out that ζ_0 is the frictional resistance (force per unit velocity) per monomer unit of a polymer segment moving against its total environment, whereas D_c is related to the frictional resistance of the polymer moving against the solvent; the latter may be described by a different mutual monomeric friction coefficient ζ_c.

The mutual diffusion coefficient is related to frictional resistance by the equation[6]

$$D_c = c(\partial\pi/\partial c)_T(1 - \bar{v}_2 c)/f \quad (1)$$

where c is the concentration of polymer in g/cm^3, π the osmotic pressure, and $\bar{v}_2$ the partial specific volume of the polymer; f, the total friction of polymer against solvent per unit volume, can be expressed as

$$f = \zeta_c N_0 c/M_0 \quad (2)$$

where N_0 is Avogadro's number and M_0 the monomer molecular weight.

Since $c(\partial\pi/\partial c)_T$ has the units of an elastic modulus, the product $D_c f/(1 - \bar{v}_2 c)$ has frequently been identified as an osmotic modulus of elasticity, usually as the uniaxial compression (bulk elongation) modulus $M_{os} = K_{os} + (4/3)G_{os}$, where K_{os} is the osmotic bulk modulus and G_{os} the osmotic shear modulus, and comparisons have been made of this quantity with the conventional shear modulus G or Young's modulus E of gels measured macroscopically.[7-9] It must be emphasized that $D_c f/(1 - \bar{v}_2 c)$ represents an elasticity of the polymer being deformed independently of the solvent, as though through a semipermeable membrane,[10] and it is orders of magnitude smaller than $K + (4/3)G$ for macroscopic deformation of the entire solution or gel; K or M for any liquid or gel is at least 10^{10} dyn/cm^2. To avoid confusion, it would be very desirable to write the osmotic moduli always with a subscript, as in $K_{os} + (4/3)G_{os}$.

In the study reported here, quasi-elastic light scattering measurements have been made on semidilute solutions of gelatin and the corresponding gels that are formed from these solutions at lower temperatures. Although gelatin is a poor choice of polymer because of its complex structure, uncertain gelation mechanism, and broad molecular weight distribution, it behaves above the gel temperature as a random coil polymer[11] and the viscoelasticity of its gels corresponds to that of a network of flexible strands.[12] In the present study, it has the unique advantage that viscoelastic measurements[12] of the same gels have previously provided values of the monomeric friction coefficient ζ_0 as well as accurate values of the macroscopic shear modulus G, so the relation between scattering and mechanical measurements can be examined. From the scattering measurements on solutions above the gel temperature, the mutual diffusion coefficient D_c is determined as well as a much smaller diffusion coefficient D_2, which can be identified as the self-diffusion coefficient of the polymer. For the gels, only D_c is obtained, and its dependence on temperature and solvent viscosity (varied over a wide range by incorporation of glycerol up to 91% by weight) is examined. Over the range studied, both the friction coefficient ζ_0 and the shear modulus G were previously observed to depend on both these variables.[12]

Experimental Section

Materials. The gelatin (pigskin) was the same sample used in the previous investigation of viscoelastic properties[12] and had been provided by Rousselot S.A., Paris. Its ash content was less than 0.6%. Its isoelectric point was 7.0, the pH of an aqueous solution was 5.1, and the number-average molecular weight ($\bar{M}_n$) as determined by gel permeation chromatography on Sepharose at Rousselot was 35 000. The intrinsic viscosity $[\eta]$ in water at 35 °C was determined in our laboratory to be 22 mL/g. The molecular weight and $[\eta]$ are relatively low and reflect a substantially degraded sample. From experience with similar gelatins,[11] the molecular weight distribution is probably rather broad.

The solvents were water and glycerol–water mixtures containing 60, 73, and 91% glycerol by weight. Viscosities (η_s) and densities of these mixtures at different temperatures were taken from data in the literature;[13] several densities were checked experimentally. All the gels were made up to contain 15.0% gelatin by weight. The "dry" gelatin was first swollen in the appropriate amount of water (taking into account that the gelatin itself contained 12% residual water), the appropriate amount of glycerol was added, and the mixture was warmed and stirred gently until dissolution

0024-9297/83/2216-0441$01.50/0

was complete. The higher the glycerol concentration, the higher the temperature and the longer the time which was required; a maximum was about 16 h at 90 °C. A test of agarose gel electrophoresis[14] on samples before and after this treatment revealed no difference in migration rate, so it was concluded that no significant additional molecular degradation had occurred. Gelatin concentration (c) in g/cm^3 was calculated by assuming additivity of gelatin and solvent volumes, taking the gelatin density as 1.465 g/cm^3.

Prior to the quasi-elastic light scattering measurements, the warm solutions were filtered through Gelman Metricel 0.45-μm filters into 10-mm polished cylindrical scattering cells. In experiments above the gel temperature, the samples were held at 35.0 ± 0.3 °C, usually for at least 2 h prior to the measurements, which were made at the same temperature. In experiments on gels, each sample was kept at 0 °C for 5 h and then equilibrated for 15 ± 2 h at the desired temperature for the measurements. Some small air bubbles were trapped in the more viscous samples but in general the solutions and gels were clear.

Methods. The quasi-elastic light scattering was measured with a 64-channel real-time autocorrelator (K7025; Malvern Instruments, Ltd., Malvern, Worcs., U.K.) connected to a commercial goniometer (Malvern RR103).[15] The autocorrelation function of the scattered incident light from an argon laser (Lexel 75-.2) of wavelength 514.5 nm was acquired as a function of scattering angle from 30° to 135° with a selected photomultiplier tube (ITT FW 130) operated in a photon-counting mode. The addition of a temperature control coil to the goniometer sample holder allowed temperature regulation in the range 5–35 °C to better than ±0.2 °C. An Apple II microcomputer (Apple Computer, Inc., Cupertino, CA) interfaced to the correlator provided data storage and preliminary analyses. Subsequent detailed fittings to various model functions were performed by using nonlinear regression routines on a Harris/7 minicomputer.

The normalized intensity autocorrelation function for homodyne detection arising from a single diffusive process with the decay constant Γ can be written as[1]

$$g^{(2)}(\tau) = G^{(2)}(\tau)/\beta = 1 + Ae^{-2\Gamma\tau} \quad (3)$$

with $\Gamma = D\kappa^2$, where A is an instrument optical constant, D is the diffusion coefficient, and κ is the magnitude of the scattering wave vector, defined as $(4\pi n/\lambda_0) \sin(\theta/2)$, with n the refractive index of the medium, λ_0 the incident wavelength in vacuo, and θ the scattering angle. $G^{(2)}(\tau)$ is the unnormalized experimental autocorrelation function, and the normalization constant β for $g^{(2)}(\tau)$ is chosen as

$$\beta = \lim_{\tau \to \infty} G^{(2)}(\tau) \quad (4)$$

Although eq 3 well describes the scattering from noninteracting monodisperse particles, it is found to be inadequate for the gelatin samples described here.

In the case of gel samples the light is scattered extensively by trapped dust particles, microscopic bubbles, and other inhomogeneities that are inevitably present, and to a smaller extent by the concentration fluctuations that are of interest. The inhomogeneities in a gel are assumed to be static on the time scale of the concentration fluctuations and thus mixing of light scattered by the two sources will give a heterodyne signal of the scattering from concentration fluctuations. Then the appropriate equation for a single diffusive process is

$$g^{(2)}(\tau) = G^{(2)}(\tau)/\beta = 1 + Ae^{-\Gamma\tau} \quad (5)$$

The assumption of heterodyne detection was confirmed by observing that there was no change in the measured decay constant when a macroscopic inhomogeneity was deliberately introduced into the scattering volume. An example of a typical autocorrelation function for the scattering from a gel is shown in Figure 1, where the curve through the points is the result of a single-exponential fit using eq 5, which was sufficient to analyze the scattering from all gel samples studied here. Because of the wide range of the solvent viscosity adjusted by the glycerol concentration (0, 60, 73, and 91%) at three different temperatures (5, 12, and 20 °C), the required correlator sample times (or delay times) $\Delta\tau$ ranged from 5000 to 0.5 μs and yielded decay constants Γ from 2 to 4 × 10^4 s^{-1}. For sample times below 1 μs it was often

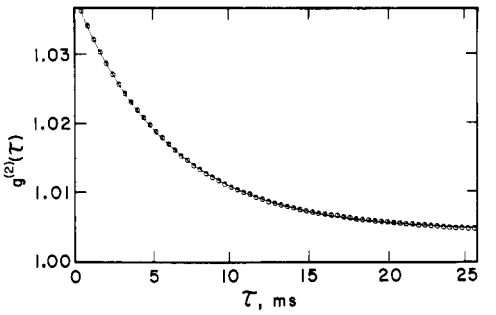

Figure 1. Plot of normalized autocorrelation function for a gel, c = 0.184, glycerol concentration 73%, at 12 °C.

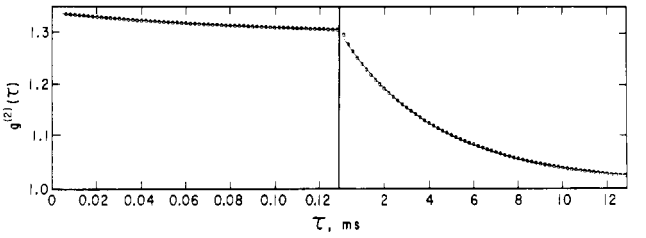

Figure 2. Plot of autocorrelation function with two time scales, normalized by a single long-time value, for a solution at 35 °C, c = 0.103 g/cm^3. Sample time: 2 μs at left, 200 μs at right. Each curve is a single-exponential fit.

necessary to delete 1–3 points at the beginning of the autocorrelation function due to errors in the detection electronics. As will be shown in the next section the calculated decay constants gave linear plots against κ^2.

For the gelatin samples at temperatures above the melting point, the quasi-elastic light scattering was more complicated and required a different scheme of data acquisition and analysis. These experiments performed at 35 °C on water solutions of gelatin at concentrations from 0.020 to 0.213 g/cm^3 showed two clearly distinguishable decays. Figure 2 demonstrates this observation. On the left half of the figure the initial fast decay is shown as acquired by the correlator with a sample time of 2 μs. In the middle of the figure the time scale changes to show the second decay, which was obtained with 200 μs as the sample time. Even though these correlation functions were measured at different times, it was possible to maintain the experimental conditions such that they can be so spliced together. After the curves are spliced, it is possible to represent the normalized autocorrelation data as

$$g^{(2)}(\tau) = 1 + Ae^{-\Gamma_f\tau} + A'e^{-2\Gamma_s\tau}$$

where Γ_f and Γ_s are the decay constants of the fast and slow processes, respectively, and A and A' are the corresponding amplitude factors. There are three limiting values of $g^{(2)}(\tau)$: $g^{(2)}(0) = 1 + A + A'$, $g^{(2)}(\infty) = 1$, and $g^{(2)}(\tau_{int}) = 1 + A'$, where τ_{int} stands for the intermediate τ (~0.2 ms) when the fast process has decayed to an apparent asymptote in the fast-time scale while Γ_s is so small that the second exponential term remains sensibly constant at A'. Thus the left portion of Figure 2 decays to $1 + A'$ while the right portion starts at the same point and decays to 1. Since Γ_f and Γ_s are well separated, it is possible to fit each set of data with an independent exponential decay as is shown by the two curves in Figure 2. The slow decay was fit with eq 3 as a single exponential with β as given in eq 4. The fast decay was likewise fit with eq 5 but β was allowed to float up to a value consistent with the complete decay of the fast exponential, that is $g^{(2)}(\tau_{int})$, in order to remove the effect of the slow process.

When a pair of scattering diffusive processes is as well separated in time scale as here, the fast process is generally detected by heterodyne signal whereas the slow process is detected by homodyne signal provided the fast and slow processes give rise to the weak and strong scatterings, respectively. This occurs because the slow-process scatterers serve as the local oscillators for the fast-process scatterers, resulting in heterodyne beating, while there no longer exist such oscillators for the slow-process scattering, so it occurs by homodyne beating. Empirically this conclusion

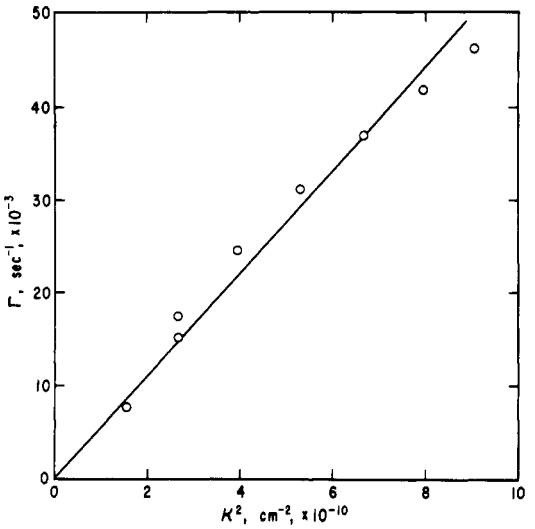

Figure 3. Plot of Γ against κ^2 for the fast mechanism of a solution at 35 °C, $c = 0.157$ g/cm^3, with a single-exponential fit of autocorrelation functions; heterodyne detection assumed. Sample times from 1 to 8 μs.

has been confirmed[16] by performing scattering experiments where 49- and 383-nm-radius polystyrene latex particles were first measured separately for their respective Stokes' radii by homodyne detection and subsequently a mixture of the two (10:1 by weight) was examined; in the latter, the fast process was shown to arise from the small particles by heterodyne beating and the slow process from the large particles. Since in the gelatin solutions the relative intensities, A, of the two exponentials were fairly constant with respect to scattering angle, that associated with the slow decay being at least 1.5 and usually 3–15 times larger than the other and increasing with concentration, we assume it is reasonable to assign the detection mechanisms in this manner. Though the assumption is well justified when the ratio is as large as 10 or more, it may be suspect when the ratio is as small as 1.5, where the heterodyne detection could be contaminated by homodyne beating. Such contamination would lead to seriously nonlinear plots of Γ vs. κ^2 because of changes in the relative contributions of homodyne and heterodyne scattering. Since our Γ vs. κ^2 plots are linear in all cases, we have eliminated this concern. The values of Γ plotted in Figures 2 and 4 were deduced on this basis.

Although the Γ values extracted from this fitting procedure were somewhat dependent on the choice of sample time, it was possible to obtain convergent values for both slow and fast decays. Similar Γ values were extracted by fitting autocorrelation functions with intermediate sample times to a model equation that was the sum of two exponentials, but since the convergence was less clear, this method was not generally used.

As an additional check on the determination of the slow-decay constants, second-order cumulant[17] analyses of the slow decays were also performed. For this model the normalization constant β was fixed at the value predicted by use of the monitor channels of the correlator. The consistency of the results is discussed in the following sections.

In all the scattering experiments, the incident laser light was polarized with its electric vector perpendicular to the scattering plane (vertical) and no depolarized scattering was observed.

Steady-flow viscosities of the aqueous solutions (no glycerol) were measured at 35 °C by capillary viscometry with a Cannon-Fenske 50 viscometer for the two most dilute solutions (2 and 5% gelatin) and a Cannon-Fenske 150 viscometer for the others (up to 20% gelatin). Densities were calculated by assuming additivity of volumes of gelatin and water. All solutions were equilibrated at 35 °C for at least 1 h prior to measurements.

Results

Solutions above the Melting Temperature. Measurements above the melting temperature were made only on aqueous solutions containing no glycerol. Figure 3 shows a representative plot of Γ against κ^2 for the fast decay observed with short sample times in such a solution, as in the left portion of Figure 2. It is linear within experimental error, and similar plots were obtained for other concentrations. Figure 4 shows the corresponding plot for the slow decay observed in the same solution with long sample times. Variation of the sample time over about a factor of 2 changes Γ somewhat as seen in the figure but the precision is not sufficient to examine the apparent dependence of D on sample time.

The diffusion coefficients calculated from the slopes of such plots are listed in Table I, identified as D_c and D_2 for the fast and slow mechanisms, respectively. In the latter

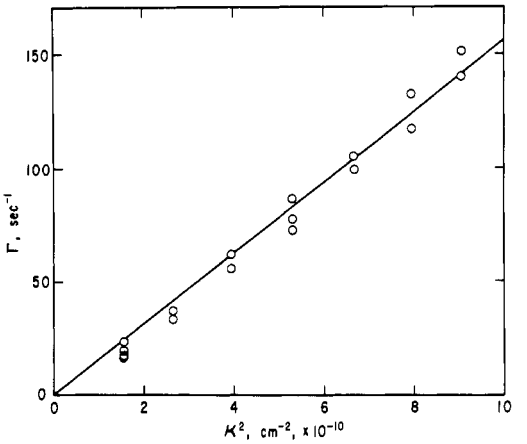

Figure 4. Plot of Γ against κ^2 for the slow mechanism of the solution of Figure 3 with a single-exponential fit of autocorrelation functions. Sample times were chosen from 200 to 2000 μs, varying by about a factor of 2 at each κ.

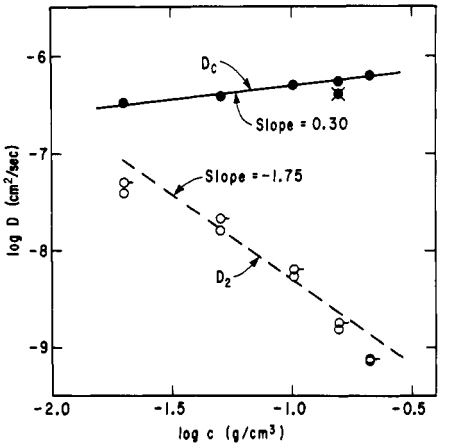

Figure 5. Logarithmic plot of D_c (fast) and D_2 (slow) against gelatin concentration for solutions at 35 °C. Points without pips, single-exponential fit to autocorrelation function; with pips, second-order cummulant model function. Point with cross, gel at 20 °C. Open circles, homodyne assumed; black circles, heterodyne assumed.

Table I
Viscosities and Diffusion Coefficients of Solutions in Water at 35 °C

wt %	c, g/cm^3	η_0, P	D_c, cm^2/s × 10^9	D_2,[a] cm^2/s × 10^9	D_2,[b] cm^2/s × 10^9
2	0.020	0.0126	328	39	50
5	0.050$_5$	0.0262	388	16.3	21.6
10	0.103	0.077	506	5.3	6.3
15	0.157	0.215	552	1.56	1.78
20	0.212	0.59	638	0.73	0.75

[a] Calculated from exponential fit of autocorrelation function. [b] Calculated from second-order cumulant fit of autocorrelation function.

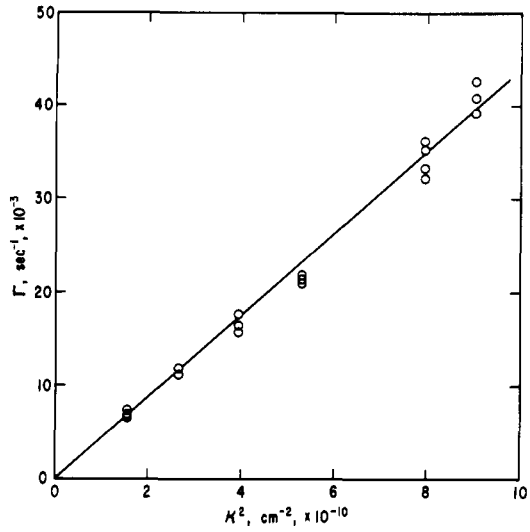

Figure 6. Plot of Γ against κ^2 for a gel at 5 °C, c = 0.156 g/cm³, water solvent, with a single-exponential fit of autocorrelation function. Sample time was chosen from 0.5 to 8 μs, varying by about a factor of 6 at each κ.

case, the calculation is based on Γ calculated both from single-exponential (as in Figure 4) and from second-order cumulant fits of the correlation function.

In Figure 5, both D_c and D_2 are plotted logarithmically against gelatin concentration. The fast diffusion coefficient, D_c, increases with concentration, approximately with the 0.3 power. This is consistent with the behavior of the mutual diffusion coefficient in a good solvent; the observed exponent is usually higher (0.7–0.8) but is smaller at lower concentrations and/or molecular weights.[4,6,18] (At low concentrations, this slope approaches zero.[4,18]) Other reasons for identifying this mechanism with the mutual diffusion coefficient D_c will be given below.

The slow diffusion coefficient, D_2, decreases sharply with increasing concentration. This is the behavior expected for the self-diffusion coefficient of the polymer; for example, the latter has been studied by forced Rayleigh scattering in solutions of polystyrene in benzene[19] and found to be proportional to $c^{-1.75}$ under conditions where entanglement was present. A line with this slope agrees approximately with the data in Figure 5 but the points show substantial curvature convex upward. Development of such curvature was observed by Hervet et al.[19] with decreasing molecular weight for solutions of polystyrene in benzene. Other reasons for identifying this with the polymer self-diffusion coefficient D_2 will be given below. (The notation follows the convention that D_1 and D_2 are the self-diffusion coefficients of solvent and polymer, respectively.) It would be expected that D_c and D_2 would converge at infinite dilution to a common value D_0; a plot with a linear c scale is consistent with this expectation.

Aggregation may be suspected as a possible explanation for our data. We have no indication of aggregation from any of the viscoelastic or light scattering measurements on the gelatin solutions prepared as we have indicated. If aggregation were responsible for the D_2 values, which range up to 500 times less than the single-particle diffusion coefficient, we would certainly expect to see aggregation effects in the correlation functions and the Γ vs. κ^2 dependence. Also, perfectly normal intrinsic viscosity extrapolations are obtained.[12] While aggregation can be a significant problem in light scattering, it is not the explanation of these results.

In one qualitative experiment on gelation kinetics, a 15% solution in water was quickly cooled from 35 to 20 °C and measurements were made repeatedly over a period of 2 h. At first, both slow and fast decays were observed, but the former disappeared within 10–15 min. (A much longer time is required for the modulus of rigidity G to approach a constant value.)

Table II
Data for Gels with 15% Gelatin by Weight

temp, °C	% glycerol	c, g/cm³	η_s, P	D_c, cm²/s × 10⁹
5	0	0.158	0.0152	436
	60	0.180	0.229	20.6
	73	0.185	0.821	4.50
	91	0.191	8.51	0.28
12	0	0.157	0.0124	432
	60	0.179	0.155	30.0
	73	0.184	0.479	6.76
20	0	0.147	0.0100	412
	60	0.179	0.108	38.8
	73	0.184	0.302	10.6

Gels. Figure 6 shows a representative plot of Γ against κ^2 for the fast mechanism observed with short sample times in a gel. Such plots were linear within experimental error and provided values of D_c. In the gels, the slow mechanism associated with D_2 does not exist, consistent with the expectation that there can be no self-diffusion of the polymer in a cross-linked structure. Values of D_c for the gels are listed in Table II together with the solvent viscosities at the respective temperatures.

In water (zero glycerol), D_c appears to decrease slightly with increasing temperature, but this is believed to be an artifact of experimental uncertainty. The average value is 427 × 10⁻⁹ cm²/s, which is somewhat smaller than the value of the corresponding solution at 35 °C from Table I, 552 × 10⁻⁹ cm²/s. However, it is clear that gelation has affected D_c very little. The point for the gel is included in Figure 5. This conclusion is similar to that reached for gel networks of a polyepoxide,[2] polystyrene,[3] and poly(dimethylsiloxane),[4] although for the latter two D_c appeared to be slightly higher in the networks than in the corresponding solutions.

In Figure 7, D_c for the gels is plotted logarithmically against the solvent viscosity η_s for all temperatures and glycerol concentrations, covering a range of 3 orders of magnitude. The plot is linear with a slope of −1.05; it is evident that within experimental error D_c and η_s are inversely proportional. (This plot ignores the expected proportionality of D_c to the absolute temperature T, but the correction would be trivial for the narrow temperature range.)

Discussion

Self-Diffusion Coefficient. For a free-draining polymer molecule without entanglements, the self-diffusion coefficient should be given by

$$D_2 = kT/P\zeta_0 \tag{6}$$

where P is the degree of polymerization and ζ_0 is the friction coefficient per monomer unit of the polymer moving through its total environment. In a 15% aqueous solution, the product $c[\eta]$ is 3.4, which is high enough for coil overlap to screen hydrodynamic interaction and to provide free-draining behavior.[20] Although screening of hydrodynamic interaction has been recently confused with entangling, it should be emphasized that the two phenomena are distinct, and the onset of the latter (entanglement regime) occurs at higher concentrations and/or molecular weights than that of the former (semidilute regime).[20-22] The degree of entanglement here should be slight if any. There is no estimate of the entanglement

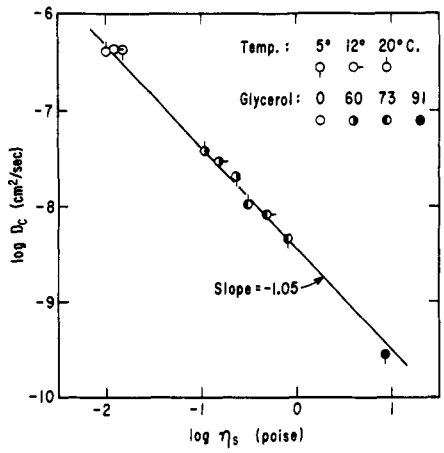

Figure 7. Logarithmic plot of D_c against solvent viscosity for gels at three temperatures and four solvent compositions.

spacing M_e of a polypeptide chain, but a representative value of 5000 for the undiluted polymer would correspond at 15% concentration to M_e = 47 000, which is above the total average molecular weight. Thus eq 6 should be applicable. The value of ζ_0 in a 15% gel has been determined from viscoelastic measurements[12] (by matching to the Rouse theory with assumption of free draining) as 3.0×10^{-8} (dyn-s)/cm at 12 °C, and it was evident from the analysis of those data that ζ_0 was proportional to η_s, so it can be adjusted (from the η_s data in Table II) to 1.74×10^{-8} at 35 °C; it should not be changed by melting the cross-links. The calculation must be very crude because of the broad molecular weight distribution, but if P is taken as 350 ($\bar{M}_n$ = 35 000, M_0 = 100 from average of amino acids[11]) we obtain from eq 6 $D_2 = 6.9 \times 10^{-9}$ cm²/s. The agreement with the observed value of 1.6×10^{-9} is quite reasonable in view of the fact that the diffusion is strongly weighted by high molecular weight species and the number-average is too small an average to use in this approximate calculation; the z average would be more appropriate. The result supports the identification of D_2 as the self-diffusion coefficient, even though it is somewhat surprising that self-diffusion should be detected in the concentration fluctuations observed by the light scattering. To the best of our knowledge, this is the first instance of the self-diffusion coefficient of a polymer chain in semidilute solution being extracted from quasi-elastic light scattering measurements, although since this paper was originally submitted similar results have been reported for polystyrene in tetrahydrofuran.[23]

From the free-draining model of the Rouse theory, D_2 can be related to the solution viscosity η_0. The steady-flow viscosity of a semidilute solution (i.e., with coil overlap and free draining but without entanglements) is calculated[24] from the Rouse theory to be

$$\eta_0 = \zeta_0 c a^2 P N_0 / 36 M_0 \qquad (7)$$

where a^2 is the mean square end-to-end distance per monomer unit; for gelatin, a can be taken[12] as 7.6 Å. Combination of this with eq 6 gives

$$D_2 = RTca^2/36M_0\eta_0 \qquad (8)$$

However, D_2 is observed to be proportional simply to η_0^{-1} instead of to c/η_0 as predicted by eq 8; this is shown in Figure 8. The value of D_2 calculated from eq 8 is fairly close to that observed at the lowest concentration but the two diverge widely at higher concentrations. This difference is not understood but cannot be attributed to the existence of entanglements, which on the basis of the reptation model would make D_2 proportional to c^2/η_0.

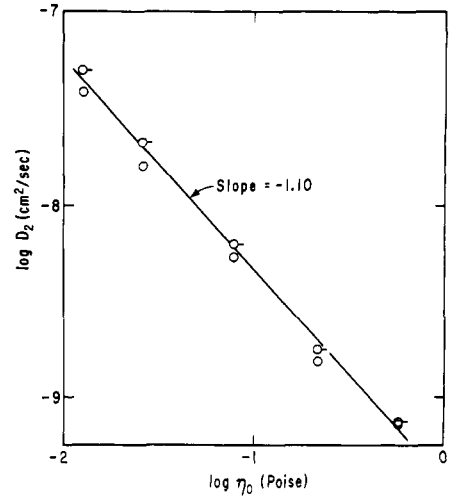

Figure 8. Logarithmic plot of D_2 against solution viscosity η_0 for solutions at five concentrations at 35 °C.

Mutual Diffusion Coefficient. At low concentrations, D_c should approach the self-diffusion coefficient at infinite dilution.[4,6,18] A very rough estimate of the latter can be made from the average hydrodynamic radius. The radius of gyration estimated from a = 7.6 Å and P = 350 on the basis of Gaussian statistics is 58 Å, which should correspond[25] to a hydrodynamic radius R_h of 46 Å. This provides $D_0 = kT/6\pi\eta_s R_h = 680 \times 10^{-9}$ in water at 35 °C, which is at least similar in magnitude to the slowly varying values of D_c plotted in Figure 4. Because of molecular weight distribution, no more quantitative comparison can be expected.

Since this paper was submitted, a brief account of the results has appeared elsewhere.[26]

Acknowledgment. This work was supported in part by the Graduate School of the University of Wisconsin, by the National Institutes of Health under Grant GM21652, and by the Polymers Program of the National Science Foundation, Grant DMR-7908652. We are indebted to Professor B. Chu for helpful comments.

References and Notes

(1) Berne, B. J.; Pecora, R. "Dynamic Light Scattering"; Wiley: New York, 1976.
(2) Jarry, J.-P.; Patterson, G. D. *Macromolecules* **1981**, *14*, 1281.
(3) Munch, J. P.; Candau, S.; Herz, J.; Hild, G. *J. Phys. (Paris)* **1977**, *38*, 971.
(4) Munch, J. P.; Lemaréchal, P.; Candau, S.; Herz, J. *J. Phys. (Paris)* **1977**, *38*, 1499.
(5) Ferry, J. D. "Viscoelastic Properties of Polymers", 3rd ed.; Wiley: New York, 1980; p 405.
(6) Sunderlöf, L.-O. *Ber. Bunsenges. Phys. Chem.* **1979**, *83*, 329.
(7) Candau, S. J.; Young, C. Y.; Tanaka, T.; Lemaréchal, P.; Bastide, J. *J. Chem. Phys.* **1979**, *70*, 4694.
(8) Hecht, A. M.; Geissler, E. *J. Phys. (Paris)* **1978**, *39*, 631.
(9) Geissler, E.; Hecht, A. M. *Macromolecules* **1980**, *13*, 1276.
(10) Hecht, A. M.; Geissler, E. *J. Chem. Phys.* **1980**, *73*, 4077.
(11) Veis, A. "Macromolecular Chemistry of Gelatin"; Academic Press: New York, 1964; pp 50 ff.
(12) Laurent, J. L.; Janmey, P. A.; Ferry, J. D. *J. Rheol.* **1980**, *24*, 87.
(13) Minor, C. S.; Dalton, N. N. "Glycerol"; Reinhold: New York, 1953; ACS Mongr. Ser. p 282.
(14) McKee, P.; Matlock, P.; Hill, R. L. *Proc. Natl. Acad. Sci. U.S.A.* **1970**, *66*, 738.
(15) Amis, E. J.; Wendt, D. J.; Erickson, E. D.; Yu, H. *Biochim. Biophys. Acta* **1981**, *664*, 201.
(16) Amis, E. J. Ph.D. Thesis, University of Wisconsin, 1981.
(17) Koppel, D. E. *J. Chem. Phys.* **1972**, *57*, 4814.
(18) Nyström, B.; Roots, J. *J. Macromol. Sci., Rev. Macromol. Chem.* **1980**, *C19*, 35.
(19) Leger, L.; Hervet, H.; Rondelez, F. *Macromolecules* **1981**, *14*, 1732.
(20) Reference 5, p 213.

(21) Graessley, W. W. *Polymer* **1980**, *21*, 258.
(22) Edwards, S. F. Reported at the U.S.-France Seminar on Polymer Solutions and Melts, Lac Du Flambeau, WI, 1980.
(23) Amis, E. J.; Han, C. C. *Polymer* **1982**, *23*, 1403.
(24) Reference 5, p 225.
(25) Schmidt, M.; Burchard, W. *Macromolecules* **1981**, *14*, 210.
(26) Amis, E. J.; Janmey, P. A.; Ferry, J. D.; Yu, H. *Polym. Bull.* **1981**, *6*, 13.

Structural Characterization of an Ethylene–Tetrafluoroethylene Alternating Copolymer by Polarized Raman Scattering

Karen Zabel,† N. E. Schlotter, and John F. Rabolt*

IBM Research Laboratory, San Jose, California 95193. *Received May 15, 1982*

ABSTRACT: The anisotropic scattering properties of a uniaxially oriented filament of an ethylene–tetrafluoroethylene (E–TFE) alternating copolymer have been investigated in order to determine the molecular conformation in ordered crystalline regions. Both a trans-planar and a 3/2-helical structure have been shown to be energetically possible in an isolated molecule and in this study the group theoretical analyses for these structures are presented. Comparison of these results with polarized Raman measurements indicates that the copolymer backbone crystallizes in predominantly a planar-zigzag structure. Observation of the low-frequency Raman-active longitudinal acoustical mode (LAM) and the correlation of its frequency position with the crystalline stem length obtained from SAXS and crystallinity measurements strongly support the trans-planar structure.

Introduction

Studies of molecular orientation in polymers can be useful in determining the conformational, crystal, and morphological structure[1-7] as well as in determining correlations between these microscopic structures and macroscopic properties. In highly oriented polymers the structural symmetry of the chain and crystal will give rise to spectroscopic selection rules that govern spectral activity in both the infrared and Raman spectrum. When several conformational or crystal structures have been proposed by other methods it is often possible to identify the correct one by using the results obtained from vibrational spectroscopy on a highly oriented sample.

Alternating copolymers of E–TFE, synthesized by radical copolymerization, were reported by Modena et al.[8] to exhibit high alternation. Subsequent studies by X-ray photoelectron spectroscopy,[9] NMR,[10] and ESCA[11] have since substantiated these results. This copolymer exhibits a high melting point and thermal stability[12] but is also interesting from a molecular point of view since the chemical repeat unit, $-CH_2CH_2CF_2CF_2-$, is a model of a head-to-head structural defect in poly(vinylidene fluoride) (PVF_2), which is known to contain 5–10% of such defect linkages.

An early investigation[13] of the crystal and molecular structure by wide-angle X-ray scattering (WAXS) indicated that the conformation was most likely planar zigzag, possibly with slight twisting, while the chains packed into either an orthorhombic or monoclinic lattice. Conformational energy calculations by Farmer and Lando[14] found that if an isolated chain was alone considered, then the minimum-energy conformation would, in fact, be a 3/2 helix rather than a trans-planar structure. Interestingly, when these chains were packed into a crystal lattice, the planar-zigzag structure became the energetically favorable conformation. Their results also indicated that five different crystal packing schemes were possible and approximately equal in energy with one being similar to that suggested by Wilson and Starkweather[13] in their original X-ray studies.

In this work the anisotropic scattering properties of a highly oriented filament of an E–TFE alternating copolymer have been determined and used together with group theoretical analyses to identify the chain conformation in the solid state. An intense low-frequency Raman band assignable to a longitudinal acoustical mode (LAM) has been observed and its polarized scattering used in conjunction with its band position as convincing evidence for a planar-zigzag conformation.

Experimental Section

The alternating copolymer of ethylene and tetrafluoroethylene used in this study was a commercial DuPont material, Tefzel 280. It was extruded and then highly drawn into an oriented transparent monofilament (by the Albany Monofilament Co.) with a diameter of 0.008 in. All Raman spectra were taken on monofilament samples as received.

The DSC melting point measurements were determined using a DuPont Model 990 thermal analyzer.

The infrared spectra of the E–TFE copolymer was obtained with an IBM 9198 vacuum Fourier transform interferometer with 2-cm^{-1} resolution. The thin-film samples for the infrared transmission studies were prepared by pressing the melted copolymer between the heated plates of a Carver press. An IR polarizer was employed to ensure that the films produced by this technique were isotropic.

Raman spectra were recorded with a Jobin-Yvon Ramanor HG-2S double monochromator using the 5145-Å line of a Spectra Physics 165-04 argon ion laser equipped with a temperature-stabilized etalon. To collect the polarized Raman spectra away from the Rayleigh line the input laser beam was passed through a 5145-Å narrow-band filter (less than 50-cm^{-1} band-pass), the polarization was selected via a polarization rotator, and the beam was passed through a Glan-Thompson polarizing prism to remove any components whose polarization may have been scrambled by passage through optical elements and finally focused on the sample. The scattered Raman signal was collected by a lens matched to the monochromator, passed through an oriented polarization analyzer, and scrambled to eliminate intensity differences due to the anisotropic diffraction properties of holographic gratings.

A conventional way to record Raman spectra of oriented filaments is schematically illustrated in Figure 1. The filament is clamped in a vertical position with the incoming laser polarization

†Summer Research Student (1981); present address: Department of Chemistry, San Francisco State University, San Francisco, CA 94132.

0024-9297/83/2216-0446$01.50/0